Proposed mechanism of kinesin backstepping

Algirdas Toleikis, Nicholas J. Carter & Robert A. Cross*

Centre for Mechanochemical Cell Biology, Warwick Medical School, Coventry CV4 7AL, UK. *Correspondence to: r.a.cross@warwick.ac.uk

Abstract

Kinesins are molecular motors that walk along microtubules, hauling cargo through the crowded cytoplasm of eukaryotic cells. At low load, kinesins almost always step towards microtubule plus ends, but at high load, forward stepping slows down and backsteps appear. Current models envisage that backsteps occur by directional reversal of the forwards walking mechanism. Here we report to the contrary, that at substall forces, kinesin steps back using a rescued detachment mechanism. We show (1) that dwell times for forward steps are shorter, on average, than dwell times for backsteps or detachments; (2) that dwell times for backsteps and detachments are indistinguishable and (3) that the balance of backsteps and detachments can be tilted dramatically, without affecting forward steps. All three points hold not only for kinesin stepping on brain GDP-taxol MTs, but also for brain GDP MTs, brain GMPCPP-epothilone MTs, *S. pombe* GMPCPP-epothilone MTs and subtilisin-treated GDP-taxol MTs. Our data establish that forward steps originate from a different and earlier state in the kinesin mechanism than the state that generates backsteps and detachments. Accordingly, we propose a model in which ATP binding to the waiting state of kinesin opens a time window exclusively for forward stepping, whilst Pi release closes this window and generates a semi-detached state which then either slips back and re-engages, completing an effective backstep, or, less usually, detaches altogether. Backstepping via this rescued detachment pathway greatly enhances kinesin's processive forwards progress under load.

Significance statement

Kinesin-1 molecular motors typically walk towards microtubule plus ends. Under load however, backsteps also occur. Backsteps have previously been thought to occur by directional reversal of forwards walking. We report that kinesin waits before forward steps for less time than before backsteps and detachments, that it waits for the same amount of time before backsteps and detachments, and that the relative numbers of backsteps and detachments can be shifted experimentally without affecting forward stepping. As we discuss, this argues for a mechanism in which motors that fail to step forward within a time window can slip back, re-engage, and retry forward stepping. Our findings speak to the mechanisms of directional bias and mechanochemical coupling in kinesins, and potentially other motors.

Introduction

Kinesin-1 is a ubiquitous, ATP-driven molecular motor that takes 8 nm steps (1) along microtubules (MTs), hauling cargo towards their plus ends. To function successfully as an intracellular transporter (2)(3), kinesin needs to move vesicles and other objects that can be several microns in diameter against appreciable hindering loads created by the crowded, and dynamic, intracellular environment. Understanding how kinesin makes consistent processive progress under dynamic load is an important problem. There is firm evidence that between steps, kinesin waits for ATP with one motor domain (the holdfast head) bound to the MT and the other motor domain (the tethered head), poised to step but prevented from doing so until ATP binds (4)(5)(6)(7)(8)(9)(10). At low hindering loads, forward steps, towards MT plus ends, predominate, whilst at higher loads, forward stepping slows down and more backsteps occur. It is clear that both forward steps (11)(12)(13) and backsteps (14)(15) require ATP and that at stall, forward steps and backsteps are equally likely (14)(15). Current models, including our own, envisage that backsteps occur by a hand-over-hand mechanism resembling that for forward stepping, but with load-dependent reversal of the directional bias (14)(15)(16)(17)(18)(19). Nonetheless, it remains possible that forwards and backwards kinesin steps occur by different mechanisms.

To test this point experimentally, we made counts of forward steps, backsteps (on average 8 nm, but up to 12 nm), larger backsteps (> 12 nm) and full detachments for kinesin stepping on GDP taxol brain MTs under defined hindering loads between 2 and 9 pN applied with an optical trap. (Fig. 1*A, B*). In a full detachment, the motor releases completely from the MT,

causing the bead-motor complex to fly back into the centre of the optical trap (Fig. 1*A*). We also compared the average dwell times for forward steps, backsteps and detachments. The dwell times are the waiting times preceding each step, consisting of the time spent waiting for ATP to bind plus the time taken to process ATP and complete the coupled mechanical step.

Average dwell times for backsteps are longer than for forward steps. Using taxol-stabilised pig brain GDP-MTs, the general form of the dwell time versus load relationship at and above stall force is as previously reported (14)(15)(16)(18), with forward step dwell times exponentially dependent on load in the region up to and including the stall force (Fig. 1*C*). Crucially however, we find that forward steps have shorter average dwell times than either backsteps or detachments (Fig. 1*C*). Previous work, including our own, has assigned backsteps and forward steps as alternative outcomes from the same state or composite state in the kinesin mechanism. Correspondingly, current kinesin schemes postulate a minimum of two bound mechanical states (Fig. 1*D*, Scheme 1). In Scheme 1, ATP binds to state 1, the waiting state, and converts it to state 2, the stepping state, which then chooses to step forward or backward, or detach, with the choice depending on load. Because forward and backsteps originate from the same state, their dwell times are drawn from the same distribution and their dwell time versus load relationships must necessarily superpose. We now find that they do not. To explain this we need an extra state, with ATP binding creating state 2, the try-forward state, and Pi release creating state 3, the backstepping and detaching state (Fig. 1*D*, Scheme 2). Scheme 2 is the minimum scheme required to produce different dwell time distributions for forward and backwards steps.

The difference between forward and backstep dwell times for GDP taxol brain MTs is just a few milliseconds at 3 pN load, increasing to several tens of milliseconds at 6 pN load (Fig. 1*C*). On other types of MT lattice, average forward and backstep dwell times are more different. We measured kinesin-1 single molecule stepping mechanics on brain GDP taxol, brain GDP without taxol, brain GMPCPP epothilone and *S. pombe* GMPCPP epothilone MTs (Fig. 2). Previous work has shown that the nucleotide state of tubulin can influence MT sliding velocity in zero load motility assays (20). Furthermore, lattice expansion and other lattice effects due to nucleotide state (21) drug binding (22) or kinesin binding (23)(24) can potentially affect kinesin binding and stepping. Under load, we find that these different lattices indeed substantially affect kinesin stepping. Most obviously, stalls last longer on yeast (*S. pombe*) MTs (Fig. 2*A*) compared to brain MTs, (Fig. 2*B*), indicating that

detachments at high force are more probable for brain MTs. In detail, we find that for all types of lattice that we tried, forward step dwell times are shorter, on average, than backstep dwell times and detachment dwell times. This holds true also for median dwell times (not shown).

Average dwell times for backsteps and detachments are the same. In contrast to the clearly different dwell times distributions for back and forward steps, average backstep and detachment dwell times are indistinguishable, reflecting that their dwell time distributions superpose, consistent with them originating from the same state (16)(18).

Forward step counts do not change with MT type; backstep and detachment counts vary inversely. Making counts of the numbers of foresteps, backsteps and detachments at each load gives further insight. The balance between backsteps and detachments shifts substantially across the different MT lattices, whilst the fraction of forward steps is little affected (Fig. 3*A*-*D*). Fig. 3*E* summarises the incidence of each event-class versus load, relative to a reference (see legend). Plotting the ratio #foresteps / #backsteps shows that this ratio decreases exponentially with load and that both the exponential factor and the stall force, the force at which the ratio is unity, are different for the different MT lattices. For GDP-taxol brain MTs, stall force is 7.3±0.2 pN as previously reported, whereas on other types of MT, stalls occur at 6.4±0.1 pN (Fig. 3*F*). By contrast, the relationship # foresteps/ (#backsteps +#detachments) versus load is almost invariant for the different types of MT (Fig. 3*G*), reflecting that the different MT lattices shift the balance between backsteps and detachments, without much affecting the count of foresteps or the total count of #backsteps + #detachments at any particular load. These data show that by varying MT type one can change the balance between backsteps, big backsteps and detachments without changing the probability of forward steps. This is only possible in the 3-state scheme (Fig. 1*D*), where backsteps and detachments branch out from state 3 and this state is different from state 2, the state from which forward steps originate. To probe the nature of state 3, we varied conditions further.

Effect of added ADP. We recorded kinesin stepping on brain GDP taxol MTs in the presence of added ADP (Fig. 4A). Adding ADP together with ATP increased the incidence of backwards events under load and dramatically increased the incidence of detachments (Fig. 4*D*). Also, the incidence of forward steps decreased, presumably because ADP competes with

ATP, and so reduces the flux through state 2. As a result, stall force is dramatically reduced, from 7.3 to 5.1±0.2 pN (Fig. 4*E*). These data indicate that adding ADP enriches state 3, from which detachments and backsteps arise. We therefore hypothesize that state 3 is a K.ADP-K.ADP state.

Effects of increased ionic strength. By increasing ionic strength, we might expect to weaken our hypothesised semi-detached K.ADP-K.ADP state, because weak binding has a considerable electrostatic component (25). We see that indeed increased ionic strength increases the incidence of detachments with much smaller effects on the incidence of backsteps and big backsteps (Fig. 4*B* and *D*), consistent with it weakening the semi-detached state and driving detachment, with a negligible effect on forward stepping. As a result, stall force is only marginally reduced (Fig. 4*E*). This is again consistent with the semi-detached state partitioning between slip-back-and-reengage events and detachment events.

Effect of subtilisin treatment. There is evidence that the binding of weak kinesin states to MTs is at least partially due to electrostatic attraction between the motor domain and the acidic C-terminal "E-hooks" of tubulin (26). Cleaving the E-hooks has only slight effects on kinesin velocity at low load, but reduces processivity (27). To further probe for our envisaged semi-detached state, we cleaved the E-hooks from GDP-taxol MTs using subtilisin, and again examined stepping mechanics. We find no appreciable effect on the tendency to take forward steps relative to all other events (Fig. 4*C* and *E*). However, we do see more big (>12 nm) backsteps and fewer detachments. This suggests cleavage of the E-hooks stabilizes the semi-detached state, allowing diffusion on microtubules over longer distances and suppressing detachment. The absence of an effect on forward stepping again shows that the balance between short backsteps, long backsteps and detachments can be tilted experimentally without affecting the forward step probability, further supporting a 3-state model.

Forward steps come from an earlier state in the mechanism than backsteps. Our findings support a scheme in which foresteps originate from a different and earlier state in the mechanism than the state that generates backsteps and detachments (Fig. 1*D,* Scheme 2). Scheme 2 is the minimum scheme required to allow different MT types to shift the balance between backsteps and detachments, without affecting forward stepping. Scheme 1 is ruled out because it predicts that whilst the choice between forward and backward steps can be load-dependent, forward and backsteps must have the same dwell times at any particular load

– and we have shown that they do not. How might scheme 2 map to the kinetic mechanism of kinesin?

Proposed Model. In our proposed scheme (Fig. 5), backsteps and detachments happen only after a failed forward step. In common with other current schemes, ATP binding opens a gateway to forward stepping by stabilising neck linker docking (28)(29)(30)(31) and triggering diffusion-to-capture of the tethered head (4)(32)(33)(5) . We propose that ATP binding opens a time window devoted *exclusively* to forward stepping. Our scheme allows for forward stepping under load from either the ATP and ADP.Pi states of the holdfast head (blue pathway). The forward-step time window is closed by Pi release (34). At high hindering loads, forward stepping increasingly fails to occur within its time window. We propose that only then, after the forward step time window is closed, can backsteps and detachments occur. Kinesins that fail to step forward within the forwards step time window switch rapidly into a semi-detached K.ADP-K.ADP state (orange pathway). We envisage that this semi-detached K.ADP-K.ADP state can slip backwards under load along the lattice, pulled by the optical trap, and then re-engage, release ADP and return to its ATP-waiting state, completing a *de facto* backstep. Re-engagement usually occurs to the neighbouring subunit, resulting in an 8 nm backward slip. Less routinely, backward slips of 16 or 24 nm occur, or the motor can fully detach. For completeness, we also show a presumptively off pathway transition, in which MT-activated ADP release occurs with the motor standing in place (grey arrows).

Relationship to other models. The K.ADP state is the weakest binding state of the kinesin motor domain (35)(36) and is usually assigned as the detaching state of the kinesin dimer (15)(10)(37). The idea that some backsteps are slips is also not novel; 16 nm, 24 nm and larger backwards displacements have previously been assigned as slips, on the basis that they are too fast to represent a sequence of 8 nm steps that are each coupled to an ATP turnover (15). The novel features of our new scheme (Fig. 5) are (1) that ATP binding opens a time window devoted to forward stepping, and (2) that all or almost all backsteps under load are backslips (rescued detachments). Our proposed rescued detachment mechanism for backsteps is consistent with recent work showing that adding Pi extends the single molecule run length of kinesin-1 (34) under forwards load, because it predicts that adding Pi will enrich the K.ADP.Pi-K.ADP state and thereby delay the formation of the backslipping K.ADP-K.ADP state. Equally, our scheme is consistent with models in which slower ATP hydrolysis promotes diffusion-to-capture by the tethered head (10)(38), because this would also extend

the time-window for forward stepping. It is possible that rescued detachments might be a more general principle of molecular motor function, important beyond the stepping mechanism of kinesin-1. For example, for kinesins working in teams, rescued detachment of the K.ADP-K.ADP state might serve to relieve internal strain within a team of collaborating motors.

Mechanochemical coupling. As with previous models, our new model (Fig. 5) implies that kinesin consumes more ATP at high loads, because backwards events consume ATP. Even an 8 nm backwards event will consume one ATP to slip backwards and another to step forward again to its original position, whilst longer backslips will require further ATP-driven forward steps to restore the motor to its starting position. In one sense, these extra turnovers are futile, because in the short term they generate negative progress. In the longer term however, such extra turnovers are far from futile, because they create the opportunity to retry forward stepping without letting go of the MT and without losing all the ground previously gained. The overall effects of our proposed rescued detachment pathway are to boost processivity and extend the total time spent trying to step forward at a particular load, with a resulting increase in the probability of successful forward steps at high load, and a consequent increase in stall force. More broadly, the biological value of our proposed slip-back-and-reengage mechanism for backsteps lies in its allowing kinesin to reduce its coupling ratio (change gear) at high loads, whilst maintaining the ability of the trailing (holdfast) head to detach rapidly should forward stepping succeed. The overall effect is to maximise processive forwards progress under load.

Materials and Methods

Kinesin-beads. Unmodified 560 nm diameter polystyrene beads (Polysciences) were mixed with purified recombinant full-length *Drosophila* kinesin-1 (12), serially diluted until only 1/3 of beads were motile. Experiments were performed in BRB80 buffer (80 mM K-PIPES (pH 7.0), 2 mM $MgSO_4$, 1 mM EGTA, 3 g/L glucose) with 1 mM ATP and glucose-catalase oxygen scavenging system and 10 µM taxol or 10 µM epothilone or with no drug.

MTs. Purified tubulin (either from porcine brain or from *S. pombe (α1, α2, β* isoforms (39)) was polymerized in BRB80 at 37°C for 45-60 min in the presence of 1 mM GTP and 2 mM

$MgCl_2$. MTs were spun down and resuspended in BRB80 supplemented with taxol (Sigma-Aldrich) or epothilone (VWR International) to 20 μM. In the case of unstabilised GDP MTs, no drug was added but MTs were capped immediately following assembly using tubulin premixed with 1 mM GMPCPP and incubated for 1 h, added to a final concentration of 1 μM. The capped MTs were spun down and resuspended in BRB80.

Flow cells. The flow cell surface was passivated with 0.1 mg/ml PLL-PEG and then with 0.1 mg/ml casein (Susos AG, Dübendorf, Switzerland). MTs were covalently attached to the coverslip surface using mild glutaraldehyde crosslinking to the APTES silanized surface (40).

Optical trapping. A custom-built optical trap (15) was used, equipped with a 6 W Nd:YAG 1064 nm laser (I E Optomech Ltd, Newnham, England). High ionic strength experiments were performed in BRB160, which is identical to BRB80 but with 160 mM K-PIPES. MTs were initially visualized by differential interference contrast (DIC) microscopy and beads moved into position above the MTs by steering the trap. Imaging was then switched to amplitude contrast and the image projected on to the quadrant photodiode detector. Data were recorded at 20 kHz and moving-average filtered to 1 kHz during analysis.

Data analysis. Data were analysed in R using custom-written code (available on request). Automated step-detection was implemented using t-test analysis. In the t-test analysis, 8 data points before the suspected step and 8 after the step were compared by t-test. The threshold t-value was set to 30 and the minimum step size to 5 nm. Dwell times were defined as the waiting time between two consecutive steps. ~30-40% of the longest dwells in each force bin were manually verified to ensure there were no undetected steps within these dwells. Only steps above 2 pN could reliably be detected and only these were processed. Below 3 pN backsteps were rare and above 8 pN forward steps were rare. For forward step:backstep ratio measurements, the force range 3-8 pN was analysed to ensure a sufficient number of both forward steps and backsteps. Each force bin includes data at the force shown ± 0.5 pN.

References

1. S. M. Block, L. S. Goldstein, B. J. Schnapp, Bead movement by single kinesin molecules studied with optical tweezers. *Nature* **348**, 348–352 (1990).

2. E. Karsenti, Self-organization in cell biology: a brief history. *Nature reviews Molecular cell biology* **9**, 255–262 (2008).

3. N. Hirokawa, Y. Tanaka, Kinesin superfamily proteins (KIFs): Various functions and their relevance for important phenomena in life and diseases. *Experimental Cell Research* **334**, 16–25 (2015).

4. D. D. Hackney, Evidence for alternating head catalysis by kinesin during microtubule-stimulated ATP hydrolysis. *Proceedings of the National Academy of Sciences of the United States of America* **91**, 6865–6869 (1994).

5. M. C. Alonso, *et al.*, An ATP Gate Controls Tubulin Binding by the Tethered Head of Kinesin-1. *Science* **316**, 120–123 (2007).

6. T. Mori, R. D. Vale, M. Tomishige, How kinesin waits between steps. *Nature* **450**, 750–754 (2007).

7. N. R. Guydosh, S. M. Block, Direct observation of the binding state of the kinesin head to the microtubule. *Nature* **461**, 125–128 (2009).

8. J. O. L. L. Andreasson, *et al.*, Examining kinesin processivity within a general gating framework. *eLife* **4**, 1166 (2015).

9. H. Isojima, R. Iino, Y. Niitani, H. Noji, M. Tomishige, The Stepping Motion of Kinesin-1. *Nature Chemical Biology* **12**, 290–297 (2016).

10. K. J. Mickolajczyk, W. O. Hancock, Kinesin Processivity Is Determined by a Kinetic Race from a Vulnerable One-Head-Bound State. *Biophysical Journal* **112**, 2615–2623 (2017).

11. W. Hua, E. C. Young, M. L. Fleming, J. Gelles, Coupling of kinesin steps to ATP hydrolysis. *Nature* **388**, 390–393 (1997).

12. D. L. Coy, M. Wagenbach, J. Howard, Kinesin takes one 8-nm step for each ATP that it hydrolyzes. *Journal of Biological Chemistry* (1999) https:/doi.org/10.1074/jbc.274.6.3667.

13. M. J. Schnitzer, S. M. Block, Kinesin hydrolyses one ATP per 8-nm step. *Nature* **388**, 386–390 (1997).

14. M. Nishiyama, H. Higuchi, T. Yanagida, Chemomechanical coupling of the forward and backward steps of single kinesin molecules. *Nature Cell Biology* **4**, 790–797 (2002).

15. N. J. Carter, R. A. Cross, Mechanics of the kinesin step. *Nature* **435**, 308–312 (2005).

16. Y. Taniguchi, M. Nishiyama, Y. Ishii, T. Yanagida, Entropy rectifies the Brownian steps of kinesin. *Nat Chem Biol* **1**, 342–347 (2005).

17. N. R. Guydosh, S. M. Block, Backsteps induced by nucleotide analogs suggest the front head of kinesin is gated by strain. *Proceedings of the National Academy of Sciences* **103**, 8054–8059 (2006).

18. Y. Taniguchi, P. Karagiannis, M. Nishiyama, Y. Ishii, T. Yanagida, Single molecule thermodynamics in biological motors. *Biosystems* **88**, 283–292 (2007).

19. N. J. Carter, R. A. Cross, Kinesin backsteps. *Biochemical Society transactions* **40**, 400–403 (2012).

20. R. D. Vale, C. M. Coppin, F. Malik, F. J. Kull, R. A. Milligan, Tubulin GTP hydrolysis influences the structure, mechanical properties, and kinesin-driven transport of microtubules. *J. Biol. Chem.* **269**, 23769–23775 (1994).

21. A. A. Hyman, D. Chrétien, I. Arnal, R. H. Wade, Structural changes accompanying GTP hydrolysis in microtubules: information from a slowly hydrolyzable analogue guanylyl-(alpha,beta)-methylene-diphosphonate. *The Journal of Cell Biology* **128**, 117–125 (1995).

22. I. Arnal, R. H. Wade, How does taxol stabilize microtubules? *Current Biology* **5**, 900–908 (1995).

23. D. R. Peet, N. J. Burroughs, R. A. Cross, Kinesin expands and stabilizes the GDP-microtubule lattice. *Nature Nanotech* **13**, 386–391 (2018).

24. T. Shima, *et al.*, Kinesin-binding–triggered conformation switching of microtubules contributes to polarized transport. *J. Cell Biol.* **217**, 4164–4183 (2018).

25. S. Uemura, *et al.*, Kinesin-microtubule binding depends on both nucleotide state and loading direction. *Proceedings of the National Academy of Sciences* **99**, 5977–5981 (2002).

26. Y. Okada, N. Hirokawa, Mechanism of the single-headed processivity: Diffusional anchoring between the K-loop of kinesin and the C terminus of tubulin. *Proceedings of the National Academy of Sciences* **97**, 640–645 (2000).

27. S. Lakämper, E. Meyhöfer, The E-Hook of Tubulin Interacts with Kinesin's Head to Increase Processivity and Speed. *Biophysical Journal* **89**, 3223–3234 (2005).

28. S. Rice, *et al.*, A structural change in the kinesin motor protein that drives motility. *Nature* **402**, 778–784 (1999).

29. A. S. Khalil, *et al.*, Kinesin's cover-neck bundle folds forward to generate force. *Proceedings of the National Academy of Sciences* **105**, 19247–19252 (2008).

30. W. Hwang, M. J. Lang, M. Karplus, Free Energy Changes During Kinesin's Force-Generating Substep. *Biophysical Journal* **98**, 369a–1 (2010).

31. B. G. Budaitis, *et al.*, Neck linker docking is critical for Kinesin-1 force generation in cells but at a cost to motor speed and processivity. *eLife* **8**, e44146 (2019).

32. D. D. Hackney, Pathway of ADP-Stimulated ADP Release and Dissociation of Tethered Kinesin from microtubules. Implications for the Extent of Processivity †. **41**, 4437–4446 (2002).

33. R. A. Cross, *et al.*, The conformational cycle of kinesin. *Philosophical transactions of the Royal Society of London Series B, Biological sciences* **355**, 459–464 (2000).

34. B. Milic, J. O. L. Andreasson, W. O. Hancock, S. M. Block, Kinesin processivity is gated by phosphate release. *Proceedings of the National Academy of Sciences of the United States of America* **111**, 14136–14140 (2014).

35. L. Romberg, R. D. Vale, Chemomechanical cycle of kinesin differs from that of myosin. *Nature* **361**, 168–170 (1993).

36. I. M.-T. Crevel, A. Lockhart, R. A. Cross, Weak and Strong States of Kinesin and ncd. *Journal of molecular biology* **257**, 66–76 (1996).

37. K. Sasaki, M. Kaya, H. Higuchi, A Unified Walking Model for Dimeric Motor Proteins. *Biophysical Journal* (2018).

38. W. O. Hancock, The Kinesin-1 Chemomechanical Cycle: Stepping Toward a Consensus. *Biophysical Journal* **110**, 1216–1225 (2016).

39. D. R. Drummond, *et al.*, Purification of tubulin from the fission yeast Schizosaccharomyces pombe. *Methods in molecular biology (Clifton, N.J.)* **777**, 29–55 (2011).

40. M. P. Nicholas, L. Rao, A. Gennerich, Covalent immobilization of microtubules on glass surfaces for molecular motor force measurements and other single-molecule assays. *Methods in Molecular Biology* (2014) https:/doi.org/10.1007/978-1-4939-0329-0_9.

41. T. Shimizu, Nucleotide specificity of the enzymatic and motile activities of dynein, kinesin, and heavy meromyosin. *The Journal of Cell Biology* **112**, 1189–1197 (1991).

42. K. J. Mickolajczyk, *et al.*, Kinetics of nucleotide-dependent structural transitions in the kinesin-1 hydrolysis cycle. *Proceedings of the National Academy of Sciences* **112**, E7186–E7193 (2015).

Acknowledgements

We thank Douglas Martin, Masanori Mishima, Douglas Drummond and Huong Thuy Vu for helpful feedback on the draft ms. **Funding:** This work was funded by a Wellcome Senior Investigator award to RAC, grant number 103895/Z/14/Z. **Author contributions:** AT performed all the experiments and analysed all the data. NC designed and built the optical trap. AT, NC and RC collaborated to design and interpret experiments and write the ms. **Competing interests:** Authors declare no competing interests. **Data and materials availability:** All data will be made available.

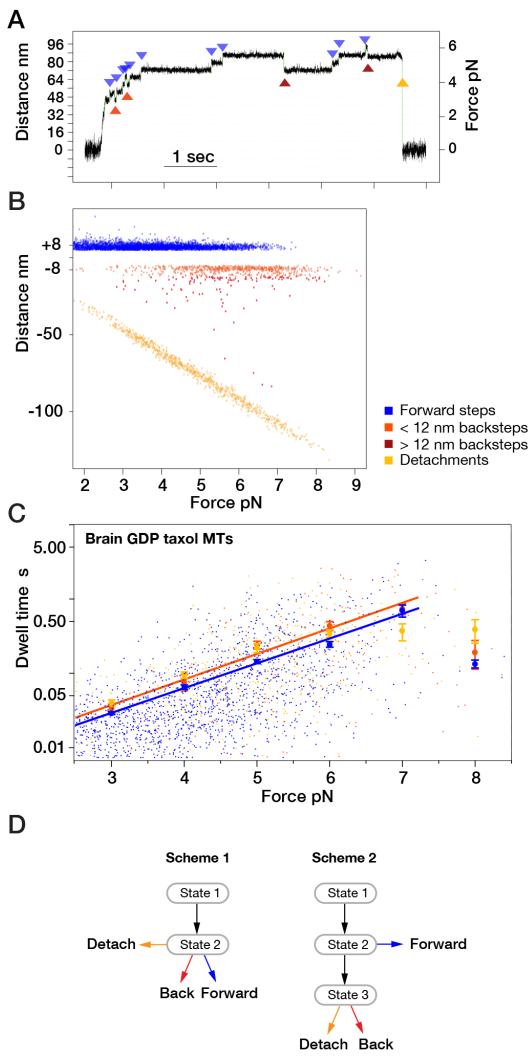

Fig. 1. Stepping of single kinesin molecules on brain GDP taxol MTs under load. (*A*) representative sequence of kinesin steps, with examples of each step-class highlighted. (*B*) Step amplitudes and incidence versus hindering force for forward steps, backsteps, larger backsteps and detachments. Trap stiffness for these experiments was ~0.06 pN/nm. (*C*) Forward step (blue), backstep (red) and detachments (yellow) dwell times vs. hindering force for Brain GDP MTs stabilised with taxol. The larger symbols are mean dwell times calculated for bins set at 1 pN intervals. Below stall, dwell times depend exponentially on load, forward step dwell times are characteristically shorter than backstep or detachment dwell times and backstep and detachment dwell times are indistinguishable. Approaching stall force on all types of MT, backstep dwell times reach a plateau, above which further increases in force have little influence on dwell time (15). Mean dwells up to the stall force (7.2 pN) were fit by least squares using log(y) = kx + b. Parameters: blue: k=0.77, b=-5.7; orange: k=0.79, b=-5.6; Errors are SEM. (*D*) Minimal schemes for the mechanical states in the kinesin mechanism (see text).

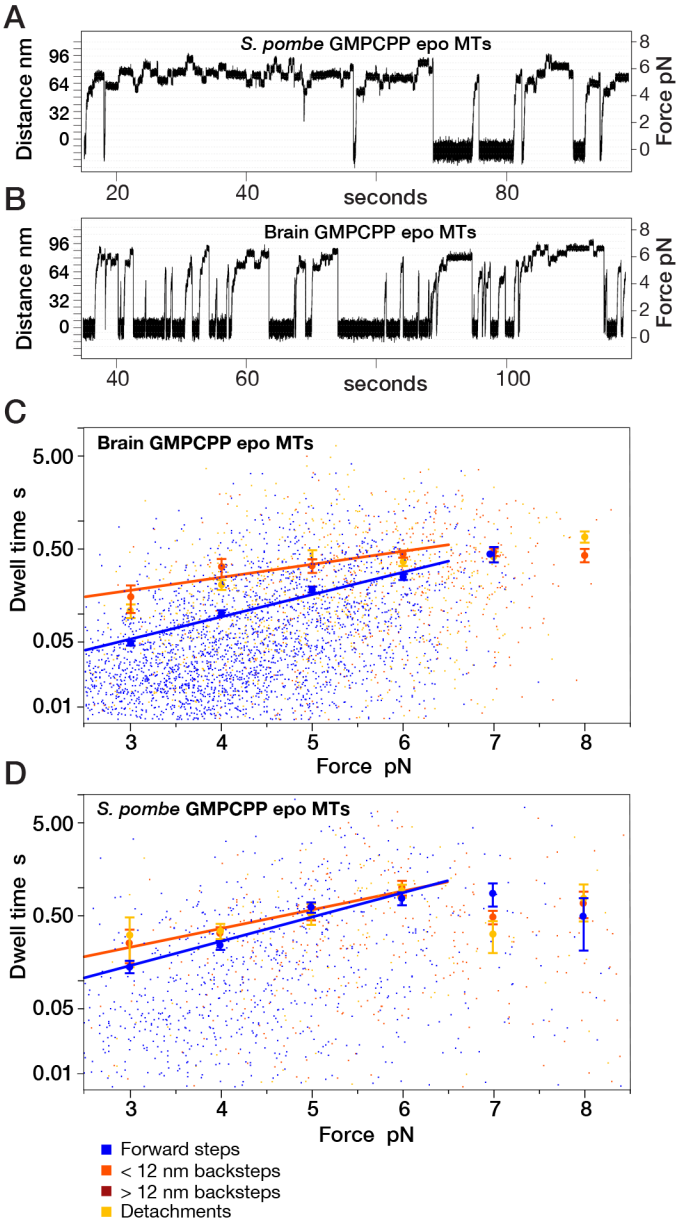

Fig. 2. Mechanics of kinesin stepping under load on different MT types. (*A,B*) typical optical trapping position versus time sequences showing the much longer stalls typically seen with *S. pombe* MTs (*A*) compared to brain MTs (*B*). (*C,D*) Dwell times versus load for kinesin stepping on (*C*) Brain GMPCPP epothilone MTs and (*D*) *S. pombe* GMPCPP epothilone MTs. As in Fig 1C, dwell times depend exponentially on load, forward step dwell times are characteristically shorter than backstep or detachment dwell times and backstep and detachment dwell times are indistinguishable. Again, approaching stall force on all types of MT, backstep dwell times reach a plateau, above which further increases in force have little influence on dwell time (15). Mean dwells up to the stall force were fit using log(y) = kx + b. Parameters: (C) blue: k=0.53, b=-4.4; orange: k=0.25, b=-2.3; (D) blue: k=0.6, b=-3.6; orange: k=0.46, b=-2.7; Errors are SEM.

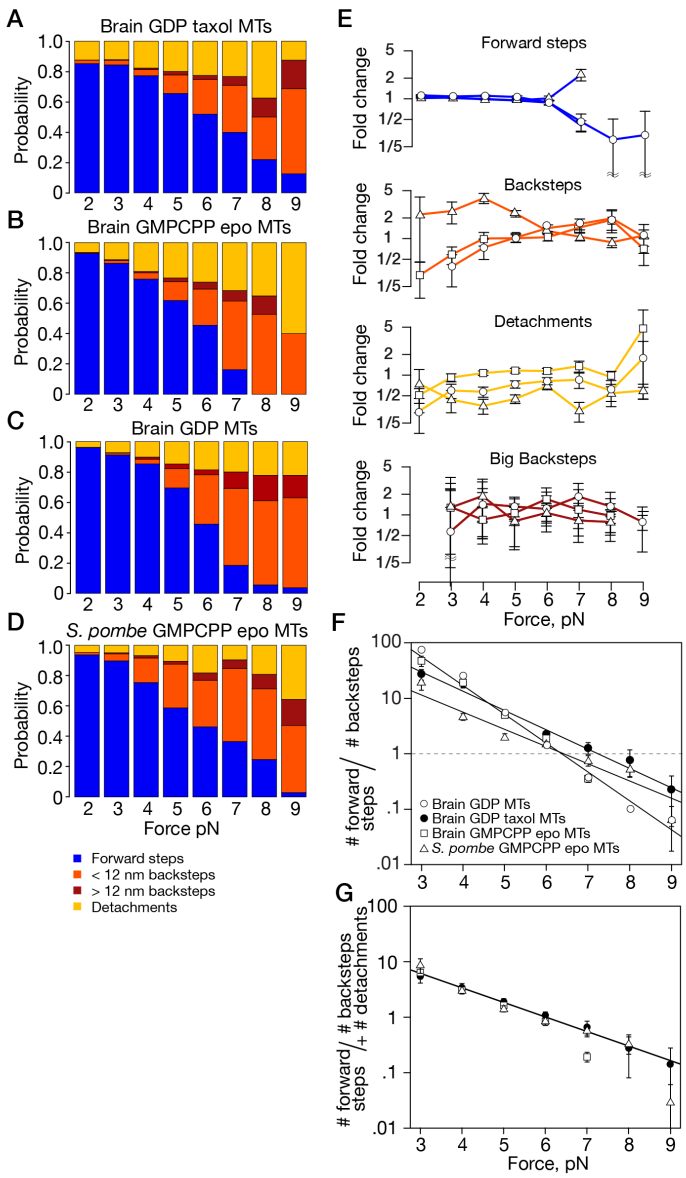

Fig. 3. Effects of changing MT type of step-event probabilities under load. (*A-D*) Probability of forward steps (blue), <12 nm backsteps (orange), >12 nm backsteps (maroon) and detachments (yellow) versus force (pN) for kinesin stepping on different MT types. (*E*) Relative probabilities for four types of event versus load, for stepping on 4 types of MT. Values are relative to GDP taxol MTs, except for *S. pombe* GMPCPP epothilone MTs, where the values are plotted relative to brain GMPCPP epothilone MTs. Errors are SE, determined by boostrapping. (*F*) #forward steps / #backsteps vs. force, for kinesin stepping on different MT types. Data were fit to log(y) = kx + b, weighting the fit by the reciprocal SEM. For brain GMPCPP epothilone MTs k=-1.16, b=7.45; for *S. pombe* GMPCPP epothilone MTs k=-0.79, b=5.0, for brain GDP taxol MTs: k=-0.83, b=5.9 . Errors are SE. (*G*) #forward steps / {#backsteps + #detachments} (including larger backsteps) versus force, for kinesin stepping on different MT types. Fit shown is to taxol data: k=-0.58, b=3.5.

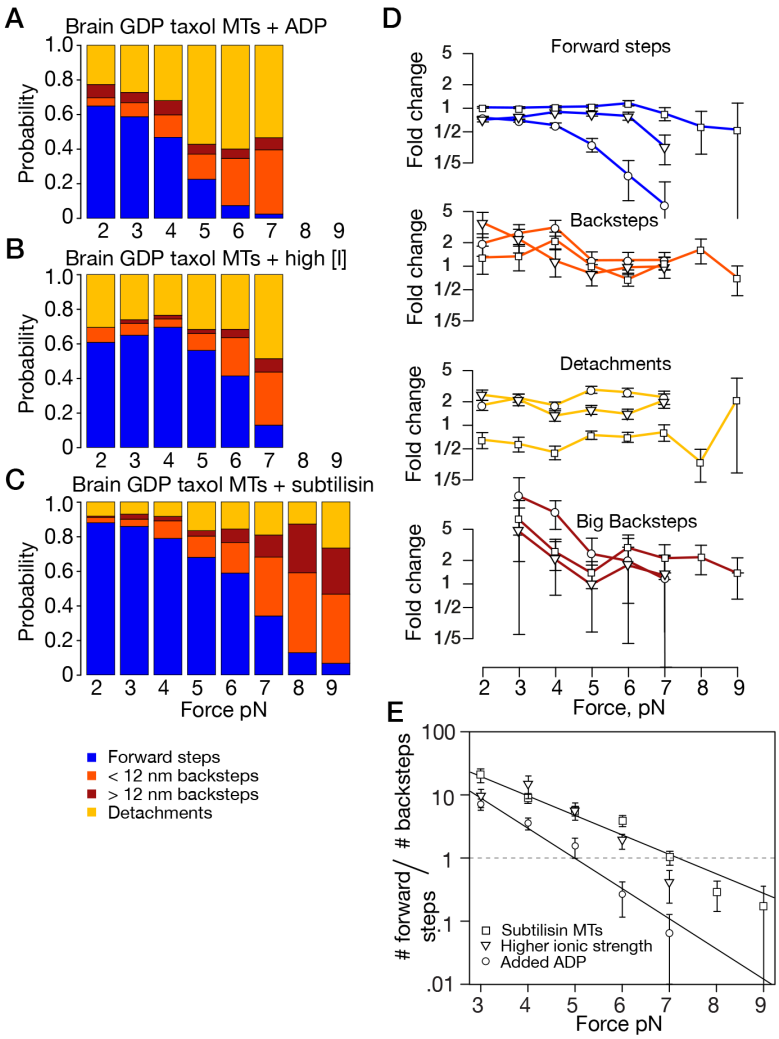

Fig. 4. Effects of changing conditions on step-event probabilities under load (*A*) Brain GDP taxol MTs with added 1mM ADP. (*B*) Brain GDP taxol MTs at higher ionic strength (BRB160 instead of BRB80) (*C*) Brain GDP taxol MTs treated with subtilisin (*D*) Relative probabilities for four types of event versus load, for stepping under these different conditions. Values are relative to GDP taxol MTs under standard conditions. Errors are SD, determined by bootstrapping. (*E*) Effect of ADP, higher ionic strength and subtilisin treatment on #forward steps / #backsteps ratio, for kinesin stepping on GDP-taxol MTs under hindering load. ADP data fit parameters: k=-0.69, b=4.9. Subtilisin fit parameters k=-0.72, b=5.1 Higher ionic strength data did not obviously fit to a single-exponential. Errors are SE.

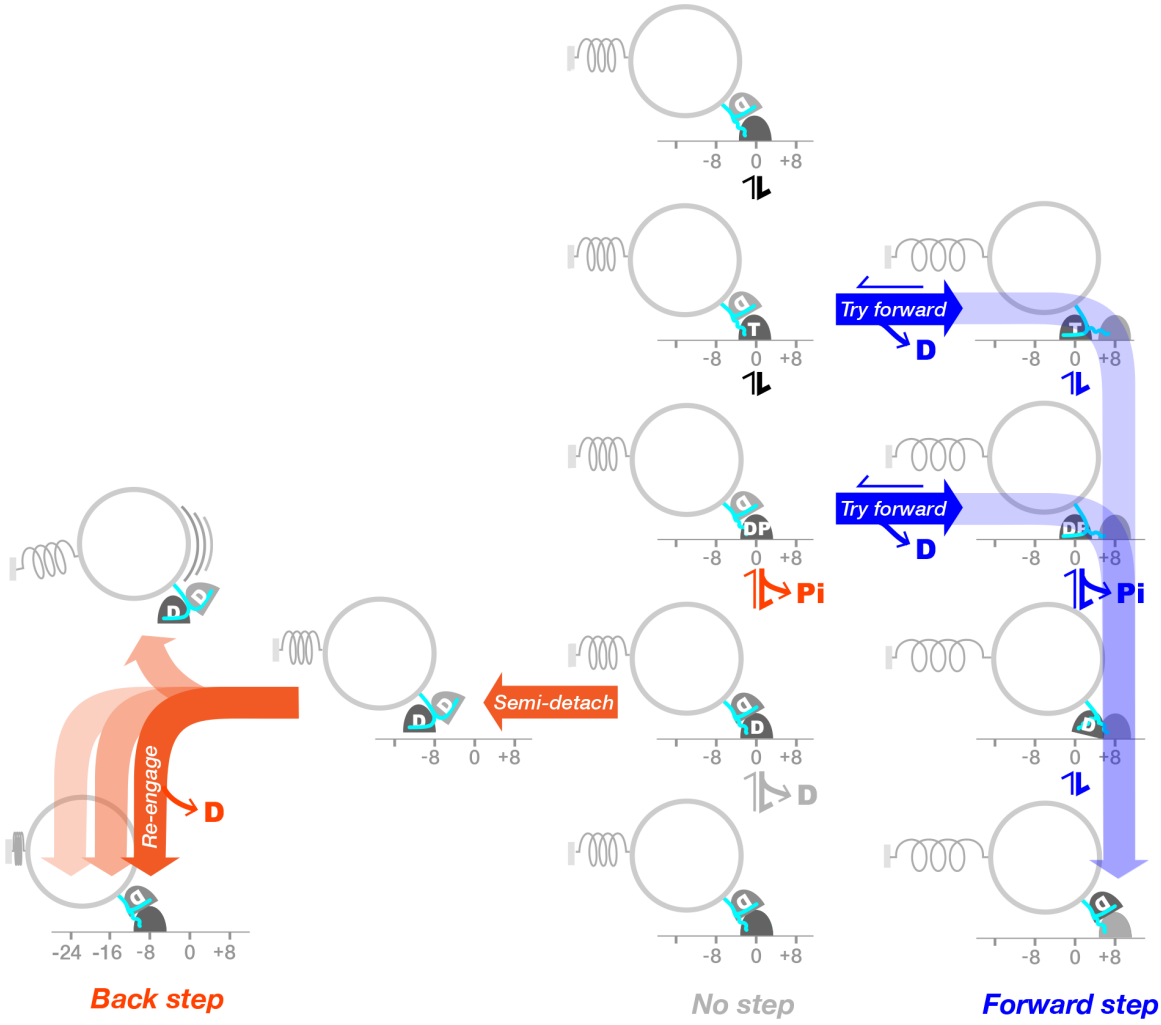

Fig. 5. Proposed model. Forward stepping takes place only within an initial era of the kinesin cycle, within a time window opened by ATP binding and closed by Pi release (blue pathway). Backwards events and detachments both originate from a K.ADP-K.ADP slip-state that arises only upon Pi release (orange pathway). For completeness a presumptively minor futile process for ADP release whilst standing still (grey pathway) is shown.